The effect of redeposition on the ion flux dependence of Si dot pattern formation during ion sputter erosion

2006 J. Phys.: Condens. Matter 18 3367

(http://iopscience.iop.org/0953-8984/18/13/004)

INSTITUTE OF PHYSICS PUBLISHING JOURNAL OF PHYSICS: CONDENSED MATTER

J. Phys.: Condens. Matter **18** (2006) 3367–3375 doi:10.1088/0953-8984/18/13/004

The effect of redeposition on the ion flux dependence of Si dot pattern formation during ion sputter erosion

Wen-bin Fan[1], Li Ling[2], Le-jun Qi[1], Wei-qing Li[1], Hai-tong Sun[1], Chang-xin Gu[2], You-yuan Zhao[1] and Ming Lu[1]

[1] Department of Optical Science and Engineering, and the State Key Laboratory for Advanced Photonic Materials and Devices, Fudan University, Shanghai 200433, People's Republic of China
[2] Department of Materials Science, Fudan University, Shanghai 200433, People's Republic of China

E-mail: minglu@fudan.ac.cn and cxgu@fudan.ac.cn

Received 31 October 2005, in final form 6 February 2006
Published 13 March 2006
Online at stacks.iop.org/JPhysCM/18/3367

Abstract

We report an ion flux dependence study of the Si dot pattern formed on Si(100) by Ar^+ ion sputtering with the ion energy being 1.5 keV, ion dose 5×10^{17} ions cm^{-2}, and ion flux ranging from 280 to 1100 μA cm^{-2}. Experimental results show that the lateral dot diameter d and the ion flux f basically follow the relationship of $d \sim 1/\sqrt{f}$, and the surface roughness w decreases with increasing f in an exponential decay manner. Simulations based on a widely accepted continuum model, namely the noisy Kuramoto–Sivashinsky equation, reproduced the trend for d versus f but failed to explain that for w versus f. A redeposition consideration was then suggested. It is found that with this correction not only are the d–f and w–f relationships well explained, but the simulated surface morphology bears closer resemblance to the experimental one as well. The effect of redeposition becomes important for $f > \sim$130 μA cm^{-2} as derived in this work.

1. Introduction

Self-organized nanodot arrays formed on solid surfaces by normal-incidence ion sputter erosion have received increasing interest in recent years for their spatially high densities, ordered distributions and cost effectiveness [1–11]. Following the Bradley–Harper (BH) theory [12, 13], this technique of ion sputtering also allows a precise control of semiconductor nanodot size through adjusting the sputtering parameters such as ion energy, sputtering temperature and ion flux, which is of significant importance in developing new optoelectronic devices based on the quantum confinement effect. Such ion energy and temperature dependences have been investigated by experiments [5, 6], which agreed well with the theoretical predictions. However, for the ion flux dependence, it was recently noticed [7, 11]

that for sufficiently low ion flux, the nanostructuring of semiconductor single crystals is not only governed by the BH theory, but the effect of the Ehrlich–Schwoebel (ES) step edge barrier [14, 15] may also be involved as well, making the experimental results deviate severely from the theory.

In this work, we investigated the ion flux dependence of Si nanodots induced by ion sputter erosion on Si(100) both experimentally and theoretically. Since the ion flux dependence of parameters in the ES model is unclear right now, to avoid ambiguity, we focused herein only on the BH model dominating regime, that is for ion flux $\geqslant$220 μA cm^{-2} [11]. Hence, the ion flux range was selected as from 280 to 1100 μA cm^{-2}. Simulations based on the noisy Kuramoto–Sivashinsky (KS) equation that contains solely the BH model reproduced the experimental relationship for the lateral dot diameter d and the ion flux f, but failed to explain that for the surface roughness w and f. We then introduced a redeposition damping term, as first proposed by Facsko *et al* [8], into the KS equation. It is found that with this correction both the d–f and w–f relationships are well explained; furthermore, the simulated surface morphology bears closer resemblance to the experimental one as well. It is further inferred that this effect of redeposition cannot be neglected as it normally is for $f > \sim$130 μA cm^{-2}.

2. Experiment

Si(100) wafers (n type, 1–9 Ω cm) were used with size of 5 × 5 × 0.5 mm^3. The Si sample was supersonically cleaned in acetone and alcohol in sequence, and then transferred into the vacuum chamber of an ion sputtering system. A Kaufman-type ion source was used for the normal-incident Ar^+ ion sputtering with ion flux ranging from 280 to 1100 μA cm^{-2}. The ion beam diameter was 50 mm, so the whole sample surface was under irradiation. The ion energy was 1.5 keV and the total ion dose was kept to be 5 × 10^{17} ions cm^{-2}. The base pressure of the vacuum chamber was better than 5 × 10^{-7} Pa, but during ion sputtering the pressure rose to 1.2 × 10^{-2} Pa due to the backfilling of argon gas with purity of 99.999%. It was found that ion sputtering could heat the sample due to thermal accumulation, rendering the sample temperature rising from room temperature to 43–150 °C, depending on the ion flux used. To keep the sample temperature constant (150 °C) during ion sputtering so as to remove possible difference in diffusion coefficients due to different temperatures, parts of the samples were mildly heated by a tungsten wire at the sample backside via thermal radiation during ion sputtering. For instance, for ion sputtering at ion flux of 280 μA cm^{-2}, the sample temperature was found to rise to 43 °C, to keep the temperature at 150 °C, additional heating was provided by the tungsten wire at an electric current of 1.6 A. Hence, for each ion flux used here, a corresponding electric current was so defined that during ion sputtering the sample temperature was maintained at 150 °C. Then in preparation of a sample under sputtering for a certain ion flux, the sample was firstly heated via the tungsten wire at its corresponding electric current, then ion sputtering was applied (for ion flux of 1100 μA cm^{-2}, no additional heating was needed). The sample temperature was measured with a calibrated thermocouple that touched the edge of the sample. The surface morphology was characterized *ex situ* with an ambient atomic force microscope or AFM (model XE-100, PSIA) at room temperature in the non-contact mode.

3. Results and discussion

3.1. Surface morphology dependence on ion flux

Figure 1 shows four AFM images of the sputtered Si(100) surfaces. From figures 1(a)–(d), the ion flux f = 280, 510, 800 and 1100 μA cm^{-2}, respectively. The image size is

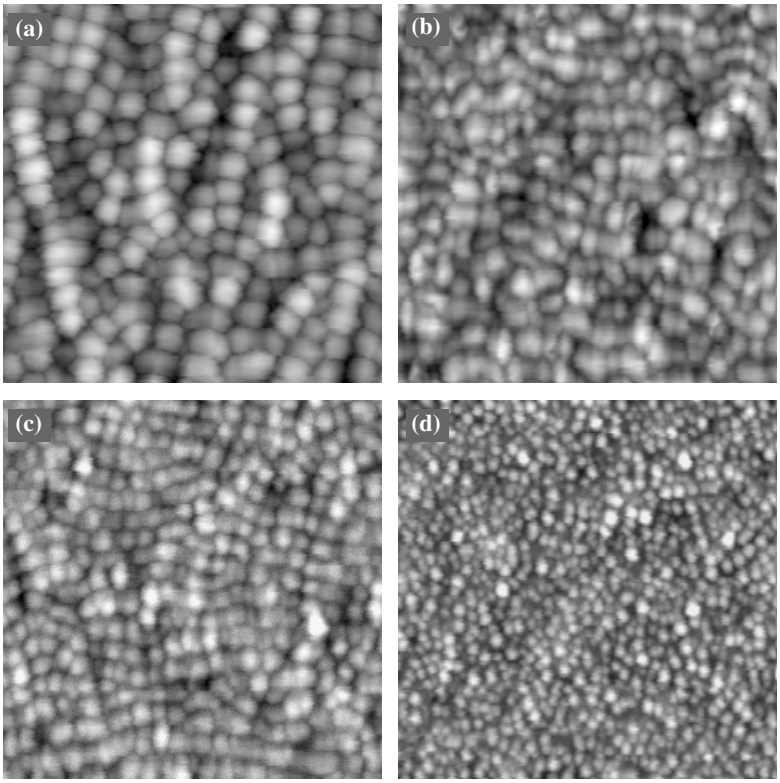

Figure 1. AFM images of Si(100) after Ar^+ ion sputter erosion. The size = 1000 nm × 1000 nm. The ion energy = 1.5 keV; ion dose = 5×10^{17} ions cm^{-2}; ion flux = (a) 280 μA cm^{-2}, (b) 510 μA cm^{-2}, (c) 800 μA cm^{-2} and (d) 1100 μA cm^{-2}.

1000 nm × 1000 nm. The details regarding the average lateral dot diameter d and the surface roughness w versus the increasing f were plotted in figures 2(a) and (b), respectively. Here w refers to the root mean square of the height difference, $h(x, y) - \bar{h}$, with $h(x, y)$ and $\bar{h}$ being the height at (x, y) on the surface and average height, respectively. Since all the sample temperatures during ion sputtering remained the same (150 °C), the difference due to temperature variation can be neglected and the evolutions of d and w are attributed wholly to the difference in f. It is seen that the data of d and w can be fitted with

$$d \sim 1/\sqrt{f}, \tag{1}$$

and

$$w \sim 1.0 + 25.4 \exp(-f/110.4), \tag{2}$$

respectively, as indicated by the solid lines in figure 2.

3.2. Simulations with the KS equation

The noisy Kuramoto–Sivashinsky (KS) equation incorporates both the BH and the ES models, and has been widely used for data analysis and simulation study [8, 10, 13, 15–17]. The KS equation that contains solely the BH model as suitable for this work is as follows:

$$\partial h/\partial t = \sum_{\vec{n}} \{-\nu_{\vec{n}} \partial^2 h/\partial \vec{n}^2 + (\partial h/\partial \vec{n})^2 \lambda_{\vec{n}}/2 - D_{\vec{n}} \partial^4 h/\partial \vec{n}^4\} + \eta(x, y, t), \tag{3}$$

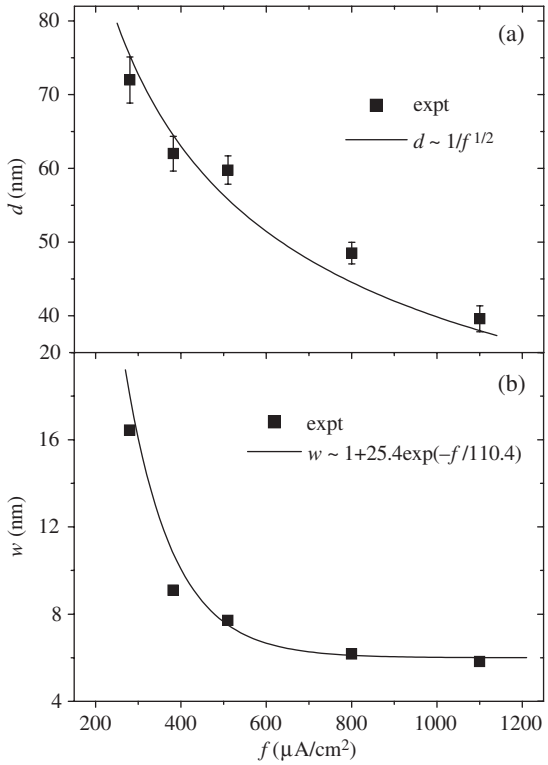

Figure 2. The measured lateral dot diameter d (a) and surface roughness w (b) versus ion flux f.

where $h(x, y, t)$ is the height of a position (x, y) on the surface at time t; $\vec{n}$ represents the crystallographic directions; $\nu_{\vec{n}}$ is the effective surface tension generated by ion sputtering, and normally temperature independent and greater than zero. The second term includes the nonlinear effect with $\lambda_{\vec{n}}$ being the tilt-dependent erosion rate, and $D_{\vec{n}}\partial^4 h/\partial\vec{n}^4$ takes into account the thermal and/or ion-induced diffusions with $D_{\vec{n}} > 0$. The last term reflects a stochastic noise. $\nu_{\vec{n}}$ is known to be proportional to f; so is $\lambda_{\vec{n}}$ [13]; thus, one may just simply change the values of $\nu_{\vec{n}}$ and $\lambda_{\vec{n}}$ at the same rate to mimic the change of ion flux. Meanwhile, for the amorphous surface as required by the BH theory, $\vec{n}$ represents two mutual-perpendicular directions such as x and y on the surface rather than crystallographic directions, and $\nu_{\vec{n}}$, $\lambda_{\vec{n}}$ and $D_{\vec{n}}$ for x and y are identical due to the surface isotropy. Hence, the subscript $\vec{n}$ can be dropped for brevity. The diffusion coefficient is taken as a constant since the thermal diffusion dominates the relaxation and the sample temperature has been held constant during ion sputtering.

The calculation was conducted by adopting the algorithm of [13]. Calculated images are presented in figure 3. To mimic the increase in f, the values of ν and λ were simultaneously varied at the same rate, hence from figures 3(a)–(d), $\nu = 0.62$, 1.00, 1.40 and 1.80, respectively; while $\lambda = 1.00$, 1.61, 2.26 and 2.90, respectively. Since in experiments the total ion dose was kept constant, the ν and the 'sputtering time' (simulation time) were so adjusted that their product remained constant when ν varied. The other parameters were identical for all, i.e. $D = 2$, time step $= 0.01$ and system image size 256×256.

The calculated relationships for d versus f and w versus f are depicted in figures 4(a) and (b), respectively. It is seen that d versus f also obeys $d \sim 1/\sqrt{f}$ (equation (1));

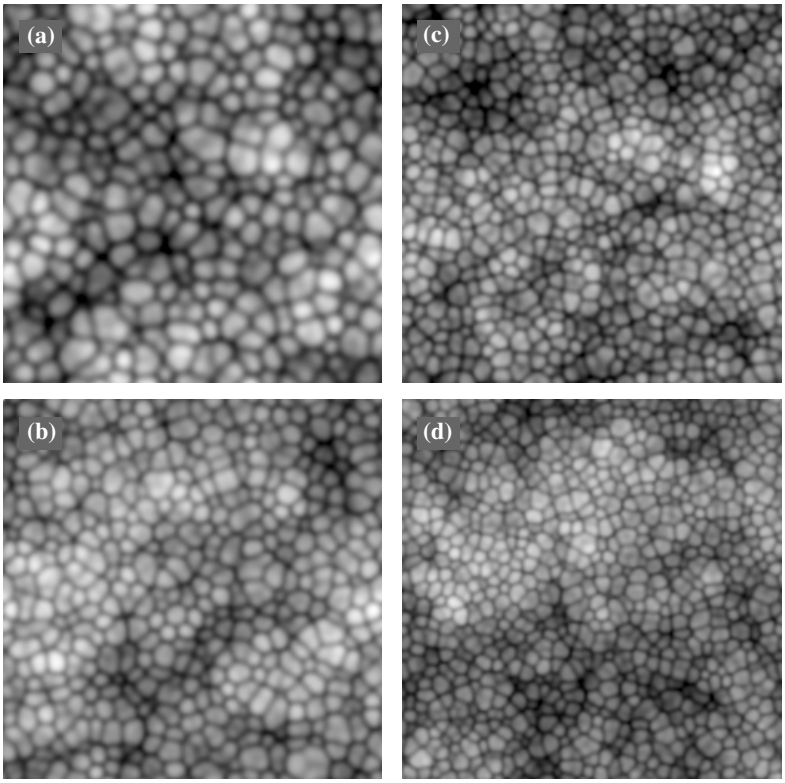

Figure 3. The simulated sputtered images. $D = 2$; time step = 0.01; system size = 256×256 and (a) $\nu = 0.62$, $\lambda = 1.00$, time = 80 500 steps; (b) $\nu = 1.00$, $\lambda = 1.61$, time = 50 000 steps; (c) $\nu = 1.40$, $\lambda = 2.26$, time = 35 600 steps; (d) $\nu = 1.80$, $\lambda = 2.90$, time = 27 800 steps.

however, the calculated relationship of w and f gives a totally different trend from equation (2). No theoretical analysis is available so far to give an expression for w versus f, but this inconsistency of the roughness data already reveals that something has been missed in the KS equation.

3.3. Simulations with the damped KS equation

In their original version of the BH theory [12], BH pointed out that the effect of redeposition of the sputtered material [8, 18] was neglected in their linear stability analysis, but if the amplitude of the disturbance has grown to a point where the nonlinear effect must be taken into account this effect cannot be ignored. Nevertheless, in the nonlinear version of BH theory developed later on [13, 16, 17] including equation (3), the effect of redeposition has still been disregarded.

Recently Facsko *et al* [8] discovered that by adding a damping term, $-\alpha h$ with $\alpha \geqslant 0$, to the right-hand side of the KS equation the calculated sputtered image is much improved and takes a striking resemblance to the experimental one of GaSb(100). They ascribed this damping term to a simple first approximation of the redeposition effect, hence the stronger the effect of redeposition, the larger the value of α is. On the other hand, Fu *et al* [18] have recently found that the depth of grooves made with a focused ion beam, decreases with increasing ion flux during the fabrication of diffractive structures. This reduction in groove depth has been attributed to the redeposition effect caused by high ion flux, and the higher the

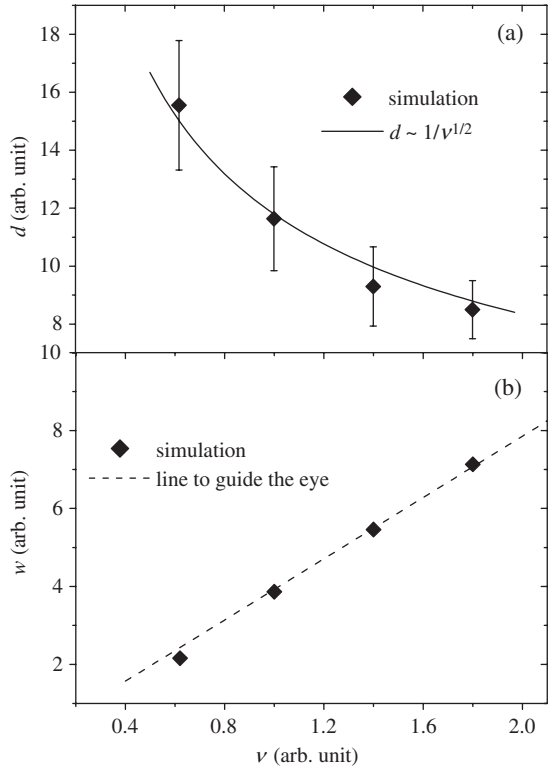

Figure 4. The simulated lateral dot diameter d (a) and surface roughness w (b) versus ν that is proportional to f; system size $= 256 \times 256$.

ion flux the stronger this effect due to the nonlinear behaviour of the groove depth with the beam current, and the small feature size of the surface microstructure. The fundamental cause for the nonlinearity between the groove depth and the ion flux arises probably from the mutual collisions among the sputtered atoms as they leave the surface. So, can the usually neglected redeposition effect be the missing term we are searching for?

We then tried to conduct simulations once again based on the *damped* KS equation by inserting the term, $-\alpha h$ into equation (3). However, such a damped equation violates the requirement of translational invariance along the erosion direction assumed by the original model [19], i.e. the equation should be independent of where the height origin is defined. In equation (3), the height actually indicates the one relative to the plane surface, rather than the one measured with respect to a height origin. From the original consideration, an additional term $-F$ should be added to the right-hand side of this equation, where F indicates the constant erosion velocity, and h is now with respect to a certain height origin. If one replaces h with $h + Ft$, then one gets equation (3) and h becomes relative to the plane surface, which still meets the requirement of translational invariance. We then modify equation (3) first by inserting $-F-\alpha(h-\bar{h})$, where $\bar{h}$ is the average surface height with respect to the height origin, then we replace $h - \bar{h}$ with h, thus the redefined height becomes relative to the average surface plane, and we finally have

$$\partial h/\partial t = -F - \alpha h + \sum_{\vec{n}} \{-\nu_{\vec{n}} \partial^2 h/\partial \vec{n}^2 + (\partial h/\partial \vec{n})^2 \lambda_{\vec{n}}/2 - D_{\vec{n}} \partial^4 h/\partial \vec{n}^4\} + \eta(x, y, t). \quad (4)$$

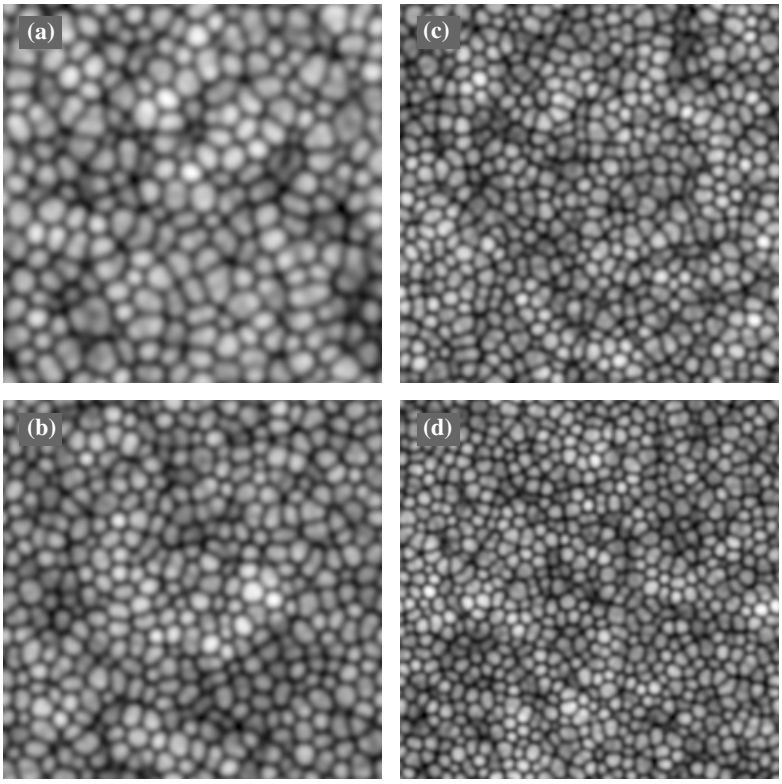

Figure 5. The simulated sputtered images after correction of the redeposition effect. All the other parameters are identical to their counterparts of figure 3, only $\alpha =$ (a) 0.02; (b) 0.075; (c) 0.154 and (d) 0.25; system size $= 256 \times 256$.

This equation remains independent of the height origin. Because $F \cdot T$ ($T =$ total sputtering time), the total etched depth, is constant throughout this work, the inclusion of the term $-F$ in equation (4) does not affect the calculated results, hence in the simulation process this term can be disregarded.

Since the detailed relationship of α and f is unknown, we determine the values of α in such a manner that with increasing f the selected set of α should yield the same expression as equation (2) for w versus f after calculating the damped KS equation. In figure 5, such recalculated images are presented. All the other parameters are identical between either image in figure 5 and its counterpart in figure 3, except that $\alpha \neq 0$ in figure 5. From figures 5(a) to (d) with the increasing ν or f, the values of α obtained by roughness data fitting are 0.02, 0.075, 0.154 and 0.25, respectively, indicating that the redeposition effect becomes stronger with increasing f, a conclusion consistent with that of Fu *et al* [18]. In figure 6, the relationships of the newly calculated d versus f and w versus f as derived from figure 5 are given. It is seen that at this time $d \sim 1/\sqrt{f}$ also holds, hence the introduction of the damping term does not affect the general lateral morphology. In fact, a close examination even reveals that after adding the damping term the calculated image is more similar in appearance to the experimental one; i.e., before the damping correction the calculated images (figure 3) are more like mosaic patterns rather than the experimentally obtained grained surfaces (figure 1), but after that (figure 5) the images become more dotted and grained. There is a similar situation in

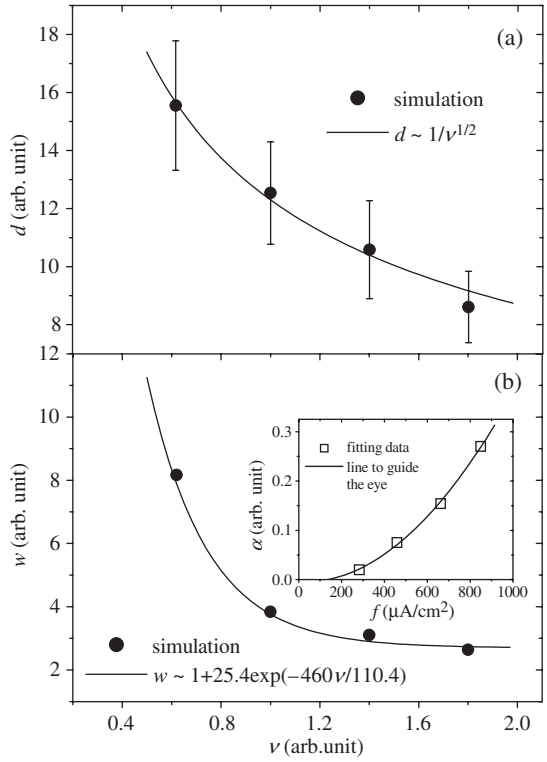

Figure 6. The simulated lateral dot size d (a) and surface roughness w (b) versus ν after the redeposition correction. The inset in (b) plots α versus f.

the case of GaSb(100) [8]. The newly calculated relationship of w and f as shown in figure 6(b) now agrees with the experimental one (equation (2)); this is natural since the set of α was so selected as described above. The α and f relationship was plotted in the inset of figure 6(b); here the value of f was obtained by the relationship of $f = 460\nu$ as acquired by fitting the w–f data with equation (2). The extrapolation shows that at $\sim$130 μA cm^{-2}, α goes to zero, and the redeposition can be ignored. It should be pointed out, however, that how precisely the damping term describes the redeposition is unknown at present, as an *ab initio* consideration of this process is lacking in the modelling work. We are only certain that qualitatively the term of $-\alpha h$ describes the redeposition correctly, and affirm the presence and importance of the redeposition effect on the nanostructuring by ion sputter erosion.

4. Summary

In summary, we have studied the ion flux dependence of Si nanodots formed by ion sputter erosion by experiments and simulations with ion flux ranging from 280 to 1100 μA cm^{-2}. The Kuramoto–Sivashinsky equation that incorporates solely the BH theory was applied to simulate the process of ion flux dependence, which explained merely part of the observed data. After adopting the correction of the redeposition effect, the simulated results agree with all the experimental ones. The results of this work should be useful in the future experimental and modelling work on the size control of Si nanodots induced by ion sputter erosion.

Acknowledgments

This work was supported by the NSFC under grant No 10374016, and the Science and Technology Commission of Shanghai under grant No 03DJ14001.

References

[1] Facsko S, Dekorsy T, Koerdt C, Trappe C, Kurz H, Vogt A and Hartnagel H L 1999 *Science* **285** 1551
[2] Frost F, Schindler A and Bigl F 2000 *Phys. Rev. Lett.* **85** 4116
[3] Gago R, Vázquez L, Cuerno R, Varela M, Ballesteros C and Albella J M 2001 *Appl. Phys. Lett.* **78** 3316
[4] Kalff M, Comsa G and Michely T 2001 *Surf. Sci.* **486** 103
[5] Facsko S, Dekorsy T and Kurz H 2001 *Phys. Rev.* B **63** 165329
[6] Lu M, Yang X J, Perry S S and Rabalais J W 2002 *Appl. Phys. Lett.* **80** 2096
[7] Ludwig F Jr, Eddy C R Jr, Malis O and Headrick R L 2002 *Appl. Phys. Lett.* **81** 2770
[8] Facsko S, Bobek T, Stahl A, Kurz H and Dekorsy T 2004 *Phys. Rev.* B **69** 153412
[9] Xu M and Teichert C 2004 *J. Appl. Phys.* **96** 2244
[10] Ling L, Li W Q, Qi L J, Lu M, Yang X and Gu C X 2005 *Phys. Rev.* B **71** 155329
[11] Fan W B, Li W Q, Qi L J, Sun H T, Luo J, Zhao Y Y and Lu M 2005 *Nanotechnology* **16** 1526
[12] Bradley R M and Harper J M E 1988 *J. Vac. Sci. Technol.* A **6** 2390
[13] Kahng B, Jeong H and Barabási A L 2001 *Appl. Phys. Lett.* **78** 805
[14] Ehrlich G and Hudda F G 1966 *J. Chem. Phys.* **44** 1039
Schwoebel R L and Shipsey E J 1966 *J. Appl. Phys.* **37** 3682
[15] Politi P and Villain J 1996 *Phys. Rev.* B **54** 5114
[16] Rusponi S, Costantini G, Boragno C and Valbusa U 1998 *Phys. Rev. Lett.* **81** 4184
[17] Valbusa U, Boragno C and de Mongeot F B 2002 *J. Phys.: Condens. Matter* **14** 8153
[18] Fu Y, Bryan N K A and Zhou W 2004 *Opt. Express* **12** 1803
[19] Barabási A L and Stanley H E (ed) 1995 *Fractal Concepts in Surface Growth* (Cambridge: Cambridge University Press)